

SUPPORTING INFORMATION

Charge carrier dynamics in tantalum oxide overlayers and tantalum doped hematite photoanodes

Tero-Petri Ruoko, Arto Hiltunen, Tomi Iivonen, Riina Ulkuniemi, Kimmo Lahtonen, Harri Ali-Löytty, Kenichiro Mizohata, Mika Valden, Markku Leskelä, and Nikolai V. Tkachenko

XPS elemental analysis

Table S1. XPS analysis for the hematite photoanodes.

Sample	Relative atomic concentration of element (at.%)										Ta/Fe (%)	
	[Component binding energy (eV)]											
	Component full width at half maximum (eV)											
	Relative atomic concentration of component (at.%)											
	C			O		N	Si	Fe			Ta	
	C 1s			O 1s		N 1s	Si 2p	Fe 2p _{3/2}			Ta 4f _{7/2}	
	C-C	C-O	C=O	O-C-O	O-M	O-Si	N-(C,O,H)	Si-O	Fe ₃ ⁺ (1)	Fe ₃ ⁺ (2)	Fe ₃ ⁺ sat.	Ta ₅ ⁺
Reference	51.3			36.0		0.6	5.3	6.7			0.0	0.0
	[285.0]	[286.2]	[287.8]	[289.0]	[529.7]	[532.2]	[399.8]	[102.6]	[710.3]	[712.5]	[719.1]	
	1.6	1.6	1.6	1.6	1.4	2.4	2.6	2.0	2.6	2.6	2.6	
	39.5	7.2	2.9	1.8	24.0	12.1	0.6	5.3	4.6	1.7	0.5	
Ta-doped	48.5			32.3		2.0	12.8	3.8			0.6	16.3
	[285.0]	[286.4]	[288.0]	[289.2]	[530.0]	[532.5]	[400.1]	[102.5]	[710.4]	[712.7]	[719.3]	[25.5]
	1.6	1.6	1.6	1.6	1.4	2.1	2.4	1.9	2.6	2.6	2.6	1.7
	36.8	6.0	3.0	2.7	14.2	18.1	2.0	12.8	2.6	1.0	0.2	0.6
Ta₂O₅-overlayer	41.3			38.6		1.1	10.8	5.2			3.0	57.5
	[284.7]	[286.2]	[287.7]	[288.9]	[529.9]	[532.2]	[399.8]	[102.3]	[710.4]	[712.6]	[719.3]	[25.6]
	1.6	1.6	1.6	1.6	1.5	2.2	2.5	2.0	2.7	2.7	2.7	1.5
	31.4	5.2	2.7	2.0	22.2	16.4	1.1	10.8	3.6	1.3	0.3	3.0

Fitting of transient absorption data

Transient absorption decay component spectra were obtained with a home-made fitting program using a Gaussian function for the instrument response function. The instrument response was not necessary for the transient absorption decays in the sub-millisecond to seconds timescale. The raw time-resolved absorption decay curves over the monitoring range were fitted globally with a multiexponential function

$$\Delta A(t, \lambda) = A_i(\lambda) \sum_{i=1}^n e^{-t/\tau_i} \quad (1)$$

where $\Delta A(t, \lambda)$ is the transient absorption with respect to time t at wavelength λ , and $A_i(\lambda)$ and τ_i are the amplitude and the lifetime of an exponential decay component, respectively. The resulting lifetime-resolved decays were plotted as decay component spectra, where each spectrum represents transient absorption change of the corresponding component with respect to wavelength. The sum of the exponential amplitudes corresponds with the change in absorption immediately after excitation. The local delay was resolved for each wavelength separately to correct for group velocity dispersion in the ultrafast measurements.

Figures

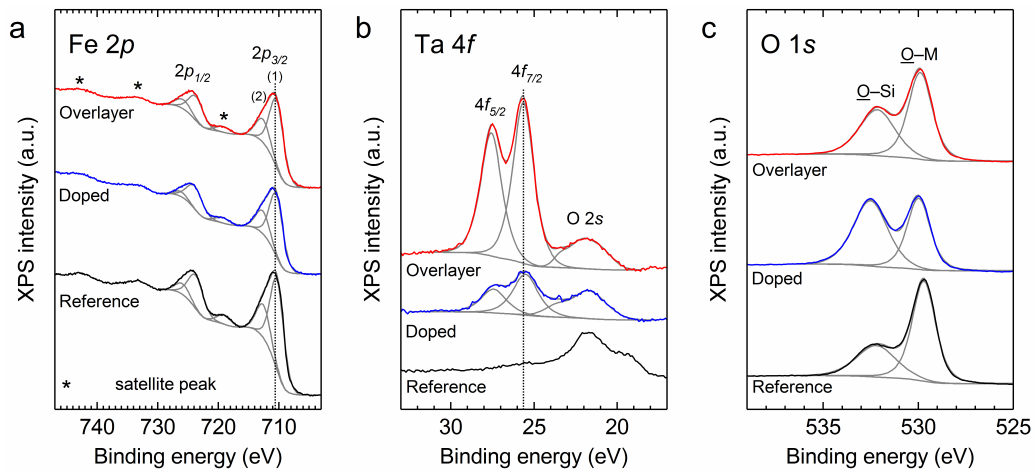


Figure S1. XPS spectra of a) Fe 2p, b) Ta 4f, and c) O 1s energy regions for the hematite photoanodes with fitted components.

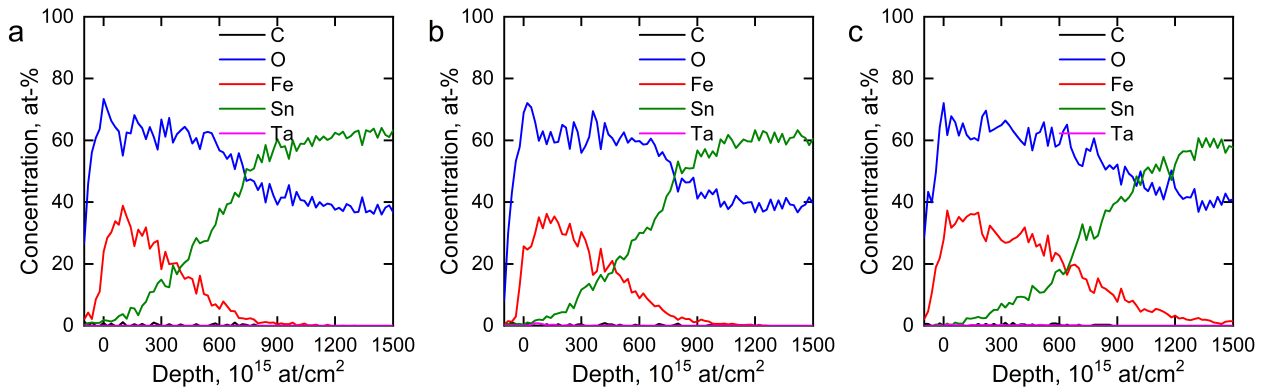


Figure S2. ToF-ERDA elemental depth profiles of a) reference, b) Ta₂O₅-overlayer, and c) Ta-doped hematite photoanodes.

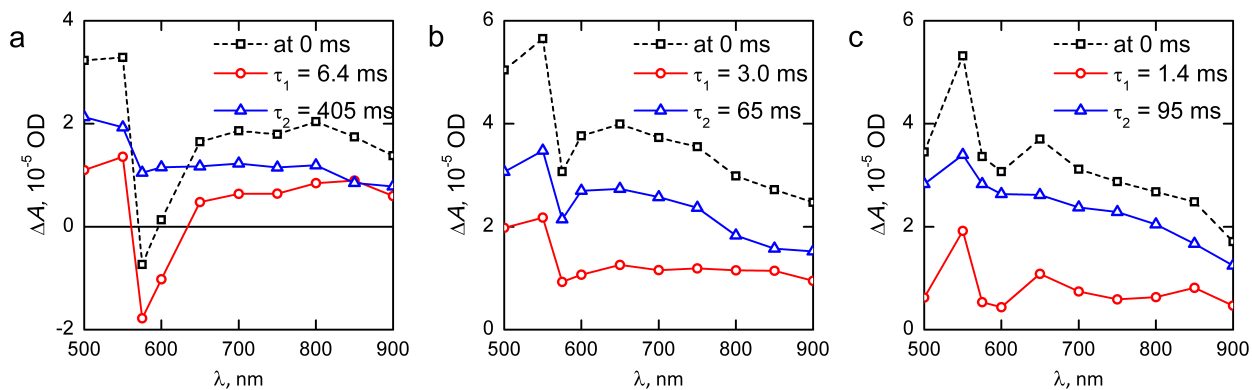


Figure S3. Biexponential decay component spectra from global fitting of sub-millisecond to second timescale transient absorption measurements of a) reference, b) Ta₂O₅-overlayer, and c) Ta-doped hematite photoanodes held at 1.60 V vs. RHE.

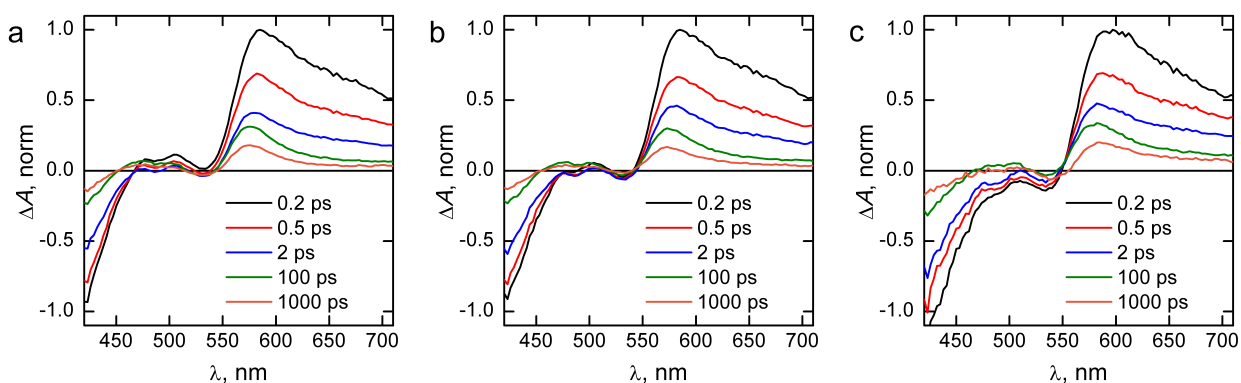


Figure S4. Normalized transient absorption spectra at selected delay times of a) reference, b) Ta₂O₅-overlayer, and c) Ta-doped hematite photoanodes in air.

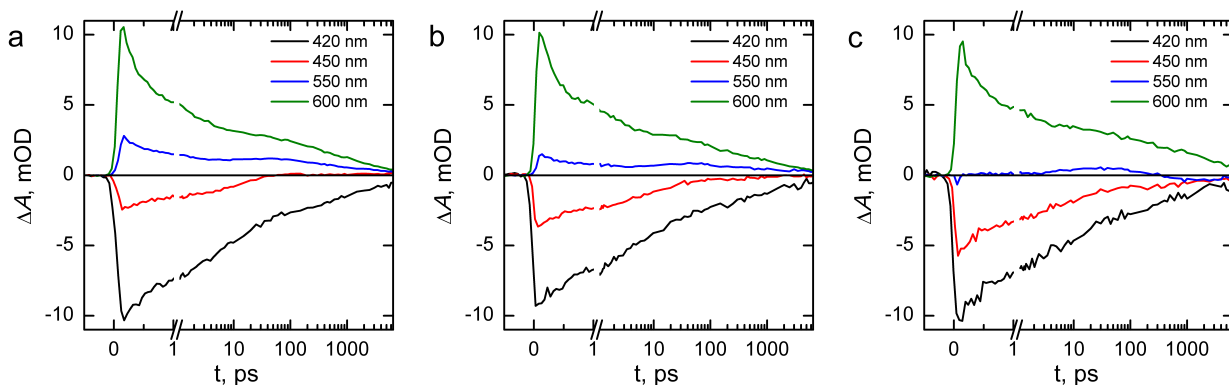


Figure S5. Transient absorption decays at selected wavelengths of a) reference, b) Ta₂O₅-overlayer, and c) Ta-doped hematite photoanodes in air, respectively. The timescale is linear until 1 ps and logarithmic for longer delay times.

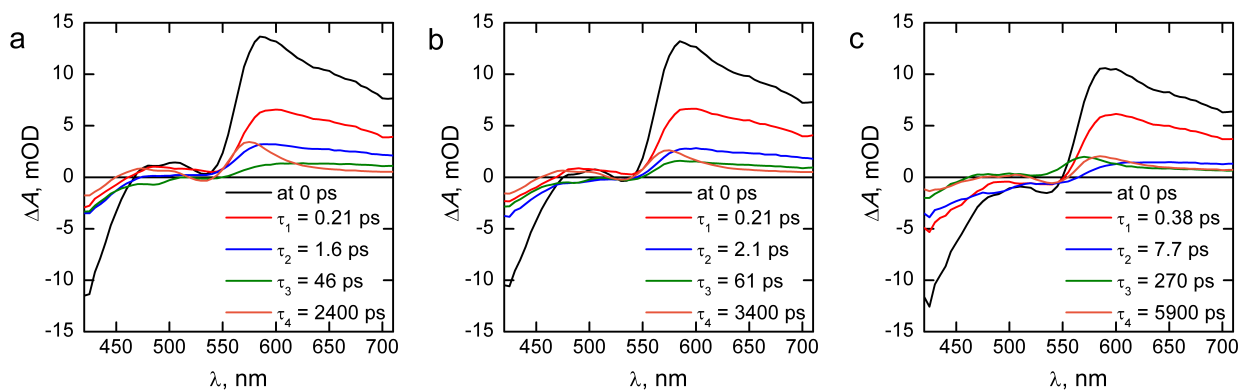


Figure S6. Four-exponential decay component spectra from global fitting of a) reference, b) Ta_2O_5 -overlayer, and c) Ta-doped hematite photoanodes in air.

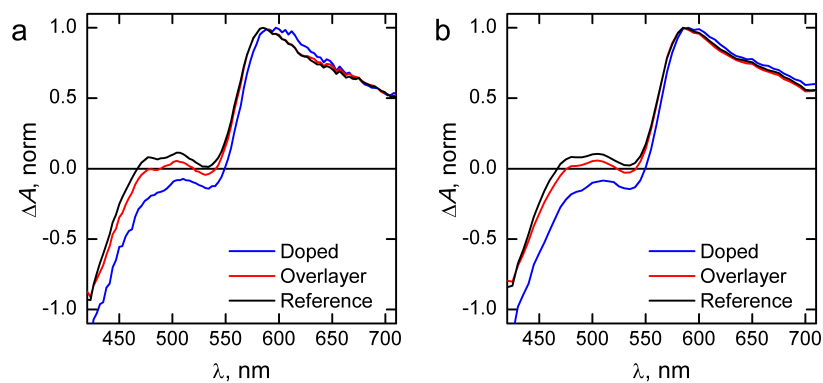


Figure S7. Normalized transient absorption spectra at a) 0.2 ps after excitation and b) immediately after excitation as obtained from four-exponential fitting.